Brain Research Bulletin 237 (2026) 111818

Contents lists available at ScienceDirect

Brain Research Bulletin

journal homepage: www.elsevier.com/locate/brainresbull

Research report

Born under a cloud: Neurophysiological consequences of maternal smoking on neonatal sleep and EEG patterns

Alja Kavčič [a,d], Jure Demšar [b,c], Maša Štihec [d], Žana Mlakar [d], Aneta Soltirovska-Šalamon [a,d,*]

[a] Devision of Neonatology, University Children's Hospital Ljubljana, University Medical Centre, Bohoričeva 20, Ljubljana 1000, Slovenia
[b] Faculty of Computer and Information Science, University of Ljubljana, Večna pot 113, Ljubljana 1000, Slovenia
[c] Faculty of Arts, University of Ljubljana, Aškerčeva 2, Ljubljana 1000, Slovenia
[d] Department of Pediatrics, Faculty of Medicine, University of Ljubljana, Vrazov trg 2, Ljubljana 1000, Slovenia

ARTICLE INFO

Keywords:
Stimulants
Child/children
High density EEG
EEG analysis
Electrophysiology
Neuroscience
Pediatrics - infants
Sleep-wake physiology

ABSTRACT

Study objectives: Sleep is a fundamental physiological process critical for central nervous system maturation and optimal cognitive development. It is known that nicotine, as a psychoactive substance, alters central signaling pathways and sleep physiology. Therefore, smoke exposure during pregnancy and breastfeeding is believed to negatively impact the newborn's sleep architecture.

Methods: In this study, we investigated the effects of indirect prenatal and postnatal nicotine exposure on sleep architecture and quantitative EEG characteristics in 28 newborns (≥37 weeks postmenstrual age), including 14 newborns born to mothers who smoked, and 14 newborns born to non-smoking mothers. Each newborn underwent a three-hour observational sleep assessment and a 64-channel EEG recording. We compared the duration of sleep stages and quantitative EEG parameters between the two groups.

Results: Newborns of smoking mothers spent a greater proportion of time in wakefulness and drowsiness and a reduced proportion in quiet sleep. Quantitative EEG analysis revealed that these newborns exhibited increased power in the theta and alpha frequency bands, decreased power in the delta frequency band, elevated spectral edge frequency (SEF 90), reduced global brain network efficiency in the alpha frequency band, and diminished fronto-temporal connectivity in the right hemisphere within the delta frequency band.

Conclusions: Our findings indicate that maternal smoking alters sleep patterns and brain activity in newborns, which could potentially have a long-term influence on central nervous system development in infancy and childhood.

1. Introduction

Nicotine exerts its neurochemical effects through interaction with neuronal nicotinic acetylcholine receptors (nAChRs), which are distributed throughout the central and peripheral nervous systems, as well as in non-neural tissues such as the placenta (Htoo et al., 2004). These receptors play a crucial role in modulating cholinergic transmission in the brain, particularly in the prefrontal cortex. Additionally, they influence catecholaminergic neurotransmission by promoting dopamine release in the nigrostriatal and mesolimbic pathways, and norepinephrine release in the hippocampus. Dopamine release has been associated with mechanisms of addiction, primarily through its involvement in arousal and reward sensation (Seth et al., 2002). Acute nicotine administration is known to alter sleep architecture, notably by increasing wakefulness and rapid eye movement (REM) sleep, while reducing slow-wave sleep (Davila et al., 1994). Studies have shown that smokers exhibit disrupted sleep macrostructure, characterized by reduced total sleep time and sleep efficiency, prolonged sleep onset latency, and a higher proportion of time spent in lighter stages of sleep (Zhang et al., 2006; Jaehne et al., 2012). However, smoking does not only affect traditional sleep architecture; it also influences more subtle changes in brain activity (referred to as sleep microstructure), which are typically observed through alterations in EEG spectral power. Research has demonstrated that smoking in adults can have long-lasting effects on brain connectivity, persisting even 20 years after sustained remission. This suggests a potentially irreversible impact of smoking on neural activity (Lee et al., 2023). Furthermore, resting-state EEG alterations have been proposed as potential biomarkers for nicotine dependence

* Corresponding author at: Department for Neonatology, University Children's Hospital Ljubljana, Bohoričeva 20, Ljubljana 1000, Slovenia.
E-mail address: aneta.soltirovska@kclj.si (A. Soltirovska-Šalamon).

https://doi.org/10.1016/j.brainresbull.2026.111818
Received 4 January 2026; Received in revised form 3 March 2026; Accepted 4 March 2026
Available online 7 March 2026

and relapse risk (Rass et al., 2016). Studies investigating passive smoking in children have reported negative effects on sleep, including prolonged sleep-onset latency, increased frequency of parasomnias, and greater daytime sleepiness (Yolton et al., 2010).

Neonates, who spend the majority of their time asleep, rely heavily on sleep for essential developmental processes. Sleep is a state of endogenously driven brain activity that supports energy conservation, neural connectivity, memory consolidation, and the development of cognitive, behavioral, and motor functions (Abbasi et al., 2023). Active sleep plays a vital role in the formation of long-term neural circuits, while quiet sleep and sleep cycling are essential for maintaining brain plasticity and processing external stimuli within the hippocampus (Dereymaeker et al., 2017). Sleep patterns—reflected in both observational parameters and EEG characteristics—serve as a valuable window into central nervous system development, evolving significantly from the preterm to term neonatal period and into infancy (Dereymaeker et al., 2017). Prenatal nicotine exposure is believed to disrupt normal sleep processes, leading to increased activity, heightened arousal, and elevated REM sleep, likely due to nicotine's excitatory effects on the reticular activating system (Stephan-Blanchard et al., 2008).

Research into neonatal sleep EEG macro- and microstructure has gained increasing importance, particularly considering findings linking sleep disturbances with poor developmental outcomes (De Beritto, 2020). Quantitative EEG measures – including signal amplitude, spectral analysis, and connectivity/network analysis – have been employed to predict neurodevelopmental trajectory and may offer additional insight into the evaluation of sleep quality (van 't Westende et al., 2022).

Despite these advances, conclusions regarding the influence of maternal smoking on neonatal sleep architecture remain inconclusive due to the limited number of studies in this area. Therefore, the present study was designed to analyze sleep patterns and quantitative EEG characteristics in newborns exposed to maternal smoking.

The present study first outlines the research methodology, encompassing behavioral sleep assessment in neonates and automated EEG sleep stage classification via computational modeling. Furthermore, it details quantitative EEG analysis techniques, specifically the computation of functional connectivity and the application of graph theory for brain network characterization. The results section elucidates

Table 1
Demographic and clinical characteristics of the subjects included in the study. M - male, F - female. The table shows that the majority of newborns had both a clinical sleep assessment and an EEG performed. For 5 participants, at the parents' request, the assessment was carried out using only one of the listed tools - patients 2, 11, 21, 25 (observation only) and patient 28 (EEG only).

Patient	Sex	Chronological age (DOL)	Diagnosis	Maternal smoking	Gestational age (weeks)	Behavioral sleep assessment	EEG
Patient 1	M	27	Congenital hydronephrosis	No	39	Yes	Yes
Patient 2	M	5	Intestinal bleeding	Yes	39	Yes	No
Patient 3	F	3	Skin hemangioma	Yes	39	Yes	Yes
Patient 4	F	28	Urinary tract infection	Yes	41	Yes	Yes
Patient 5	M	16	Laryngomalacia	Yes	40	Yes	Yes
Patient 6	M	13	Feeding difficulties	Yes	39	Yes	Yes
Patient 7	F	3	Gastroesophageal reflux	Yes	37	Yes	Yes
Patient 8	M	25	Congenital hydronephrosis	Yes	39	Yes	Yes
Patient 9	M	12	Omphalitis	No	40	Yes	Yes
Patient 10	M	9	Congenital hydronephrosis	No	38	Yes	Yes
Patient 11	M	14	Feeding difficulties	No	40	Yes	No
Patient 12	M	6	Pneumothorax (resolved, hemodynamically and respiratory stable)	Yes	39	Yes	Yes
Patient 13	M	7	Thrombocytopenia	No	41	Yes	Yes
Patient 14	M	7	Ventricular septal defect	Yes	36	Yes	Yes
Patient 15	M	19	Acute bronchiolitis	No	39	Yes	Yes
Patient 16	M	12	Esophageal atresia	No	39	Yes	Yes
Patient 17	F	11	Congenital hydronephrosis	Yes	38	Yes	Yes
Patient 18	F	15	Upper respiratory tract infection	No	37	Yes	Yes
Patient 19	M	49	Acute bronchiolitis	Yes	35	Yes	Yes
Patient 20	M	49	Acute bronchiolitis	Yes	35	Yes	Yes
Patient 21	M	26	Acute bronchiolitis with bacterial pneumonia	No	40	Yes	No
Patient 22	F	16	Early onset sepsis	No	37	Yes	Yes
Patient 23	F	12	Skin infection	No	41	Yes	Yes
Patient 24	F	15	Urinary tract infection	No	40	Yes	Yes
Patient 25	M	17	Urinary tract infection	No	40	Yes	No
Patient 26	F	9	Feeding difficulties	Yes	38	Yes	Yes
Patient 27	M	8	Transient tachypnea	Yes	38	Yes	Yes
Patient 28	F	13	Transient tachypnea	No	39	No	Yes

significant disparities in sleep architecture and electroencephalographic profiles between neonates of smoking and non-smoking mothers. Finally, the discussion situates these findings within the context of extant literature and provides a critical evaluation of the study's limitations. Main contributions and findings of the following manuscript are:

- Neonatal exposure to nicotine disrupts early sleep architecture and brain function, which reflects in quantitative EEG measures and sleep-wake cycling.
- High-density EEG seems to detect the influence of maternal smoking on brain connectivity and network characteristics in newborns.
- Changes such as reduced quiet sleep and altered EEG patterns in newborns exposed to nicotine may indicate early neurophysiological dysfunction, potentially elevating the risk of cognitive, behavioral, and developmental difficulties later in life.

2. Methods

Our aim was to assess behavioral sleep patterns, analyze sleep architecture, and evaluate quantitative EEG changes in neonates exposed to maternal smoking, and to compare these findings with neonates born to non-smoking mothers.

A total of 28 neonates (10 females) were included in the study, with the test and control groups evenly matched (14 participants in each group). Each child participated in two distinct sessions: one dedicated to behavioral observation and one for EEG recording. For 5 participants, at the parents' request, the assessment was carried out using only one of the listed tools (either observational or EEG), which is marked in Table 1. The methodology is described in detail below.

2.1. Participants

All neonates were hospitalized at the Neonatal Department of the University Children's Hospital Ljubljana for various clinical reasons between October 2024 and May 2025. Inclusion criteria for the test group were: (1) maternal smoking during pregnancy and/or during breastfeeding, and (2) a postmenstrual age of at least 37 weeks. Exclusion criteria included: (1) the presence of severe systemic diseases causing respiratory or cardiovascular instability, or (2) known neurological abnormalities, such as central nervous system malformations, congenital or acquired brain lesions, genetic syndromes, seizures, encephalopathies, or perinatal stroke syndromes.

Demographic and clinical data for all participants are presented in Table 1.

2.2. Behavioral sleep assessment

We used a sleep-scoring system for sleep stage classification in preterm infants, originally published by de Groot et al. (2022). This behavioral sleep staging system defines four sleep-wake stages: active sleep (AS), quiet sleep (QS), intermediate sleep (IS), and wakefulness (W). Classification is based on six observational parameters: eye movements, body movements (activity), facial expressions, vocalizations, heart rate, and respiratory pattern. As this scale was initially developed for preterm infants (whose sleep is more disorganized and in whom the IS stage is difficult to identify), we adapted it based on existing literature to more accurately classify the IS stage (Grigg-Damberger, 2016). Our behavioral sleep assessment protocol, based on these parameters, is shown in Fig. 1. Parameters were recorded in 1-minute intervals. When observational features did not align with a single sleep stage, we applied a classification algorithm, detailed in the flowchart (Fig. 2).

All observations were carried out by a single examiner who remained in the room with the neonate throughout the assessment. Observations were conducted in the late afternoon or evening, during periods of minimal environmental disturbance in the neonatal ward. Neonates were observed for a three-hour interval between feedings, typically capturing the transition from wakefulness at the start of the session to sleep, and returning to wakefulness by the conclusion of the observation period.

2.3. EEG recording

Twenty-four neonates underwent 64-channel EEG recording (BrainChamp, Brain Products GmbH) using R-Net caps (Brain Products GmbH) appropriately sized to the newborn's head circumference. Recordings were conducted after the newborn had fallen asleep. Observational assessments were conducted in thein a hospital bed, lasting between 20 and 40 min, and were discontinued if the newborn became restless or awoke. Only continuous, artifact-free segments were used for analysis. Segments containing significant movement artifacts were excluded. EEG data were recorded using the BrainVision software (Brain Products GmbH).

	Wake	AS	QS	IS
Eye movements	open	REM	-	opening and closing
Body movements	+	+	absent or reflexive	variable
Facial movements	+	+	-	variable
Vocalisations	+	+	-	variable
Respiratory rate	variable	irregular	regular	regular
Heart rate	variable	irregular	regular	regular

Fig. 1. Sleep stage classification system based on Behavioral Sleep stage classification for Preterm Infants. Adapted from de Groot et al. (2022). AS – active sleep, QS – quiet sleep, IS – intermediate sleep.

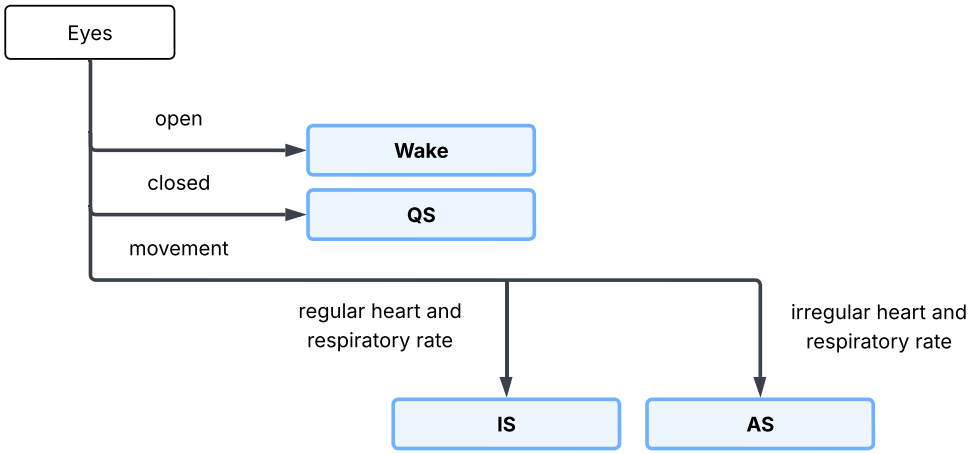

Fig. 2. Flowchart for determining sleep stages. This flowchart was used for uncertain situations, where different observed parameters did not fit into the same sleep stage category. *AS – active sleep, QS – quiet sleep, IS – intermediate sleep.*

2.4. Macrostructural sleep analysis

Sleep stages were identified using an existing automated algorithm previously applied to neonatal EEG by the Raurale et al. research group (Raurale et al., 2020). We then compared the proportion of active and quiet sleep between neonates of smoking and non-smoking mothers. To minimize movement-related noise, the first and last two minutes of each EEG recording were excluded. In accordance with prior studies, EEG data were filtered to a 0.1–30 Hz frequency range and downsampled to 64 Hz. The signals were re-referenced to the average, and a bipolar montage (F3–C3) was used. Quiet sleep was identified based on the presence of the *trace alternant* pattern. Proportions of quiet sleep were then compared between the two groups.

2.5. Microstructural sleep analysis

We further aimed to analyze quantitative EEG parameters to investigate differences between neonates of smoking and non-smoking mothers. Raw EEG data were preprocessed using the MNE-Python software package (Gramfort et al., 2013). The first and last two minutes of each recording were excluded to remove noise related to cap placement and recording termination. A band-pass filter from 0.5 Hz to 40 Hz was applied to reduce slow drift and high-frequency noise. Independent Component Analysis (ICA) and the Autoreject algorithm (Jas et al., 2017) were used to further eliminate artifacts.

2.5.1. Spectral analysis

Spectral analysis was performed using Fast Fourier Transform (FFT), which converts EEG signals from the time domain to the frequency domain, generating power spectral densities. The resulting power spectra illustrate how EEG signal power is distributed across frequency bands (delta, theta, alpha, beta, and gamma), as shown in Fig. 3.

2.5.2. SEF 90

SEF 90 is the frequency below which 90% of the brain's activity or EEG signal power is located (illustrated in Fig. 4). A high SEF 90 value indicates that higher frequencies (i.e. beta) dominate in the EEG recording. A low SEF 90 value, on the other hand, implies the prevalence of lower frequencies (i.e. delta and theta).

2.5.3. Functional connectivity between temporal and frontal brain regions

Following the signal processing procedures described above, the EEG data were segmented into 1-second epochs for analysis. These epochs were then used to assess functional connectivity between frontal and

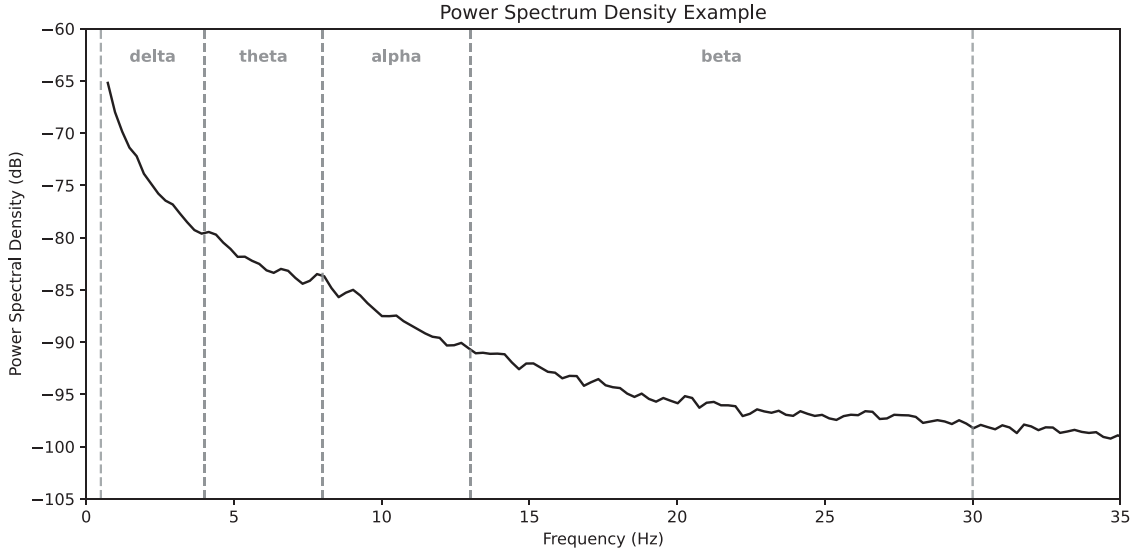

Fig. 3. An example of the power spectrum density across different frequency bands. The figure shows a decreasing power spectral density across the frequency band ranges (delta, theta, alpha, beta).

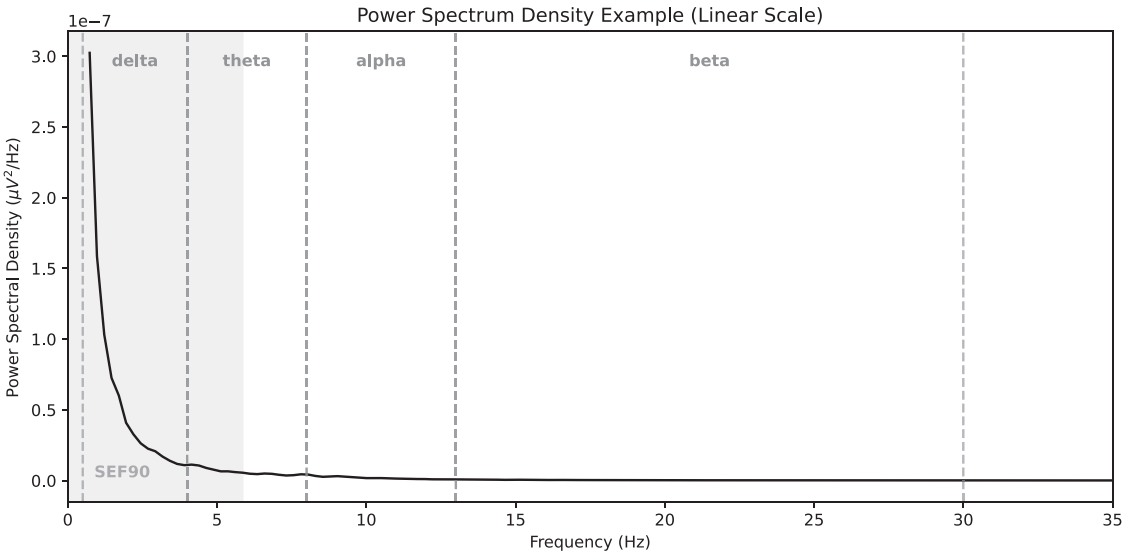

Fig. 4. SEF 90 display. The graph shows the spectral edge frequency (SEF) with a gray area, where 90% of the EEG signal's power is located.

temporal brain regions. Specifically, we evaluated signal coherence between electrodes placed over frontal and temporal areas. For the right hemisphere, the following electrodes were included: Fp2, AF4, AF8, F2, F4, F6, F8, FC6, C6, FT8, T8, and TP8. For the left hemisphere, we used:

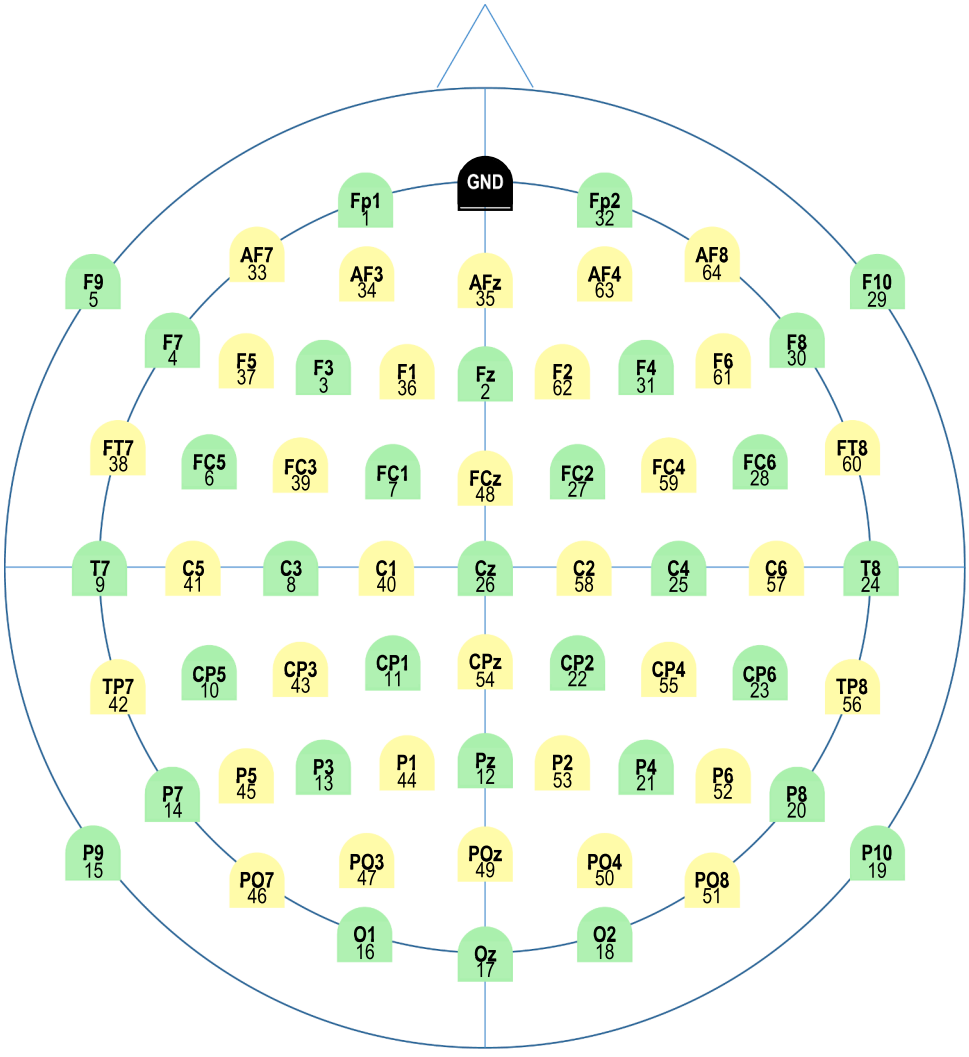

Fig. 5. Display of EEG electrodes positions. For the analysis of fronto-temporal functional connectivity, we analyzed the signal synchrony from the above-mentioned electrodes on the left and right side of the scalp. Image source: Brain Products GmbH.

Fp1, AF3, AF7, F1, F3, F5, F7, FC5, C5, FT7, T7, and TP7. The placement of all EEG electrodes is illustrated in Fig. 5.

To estimate the connectivity, we calculated the strength of the connections between two groups of electrodes (frontal and temporal). The connectivity strength (S) was calculated as:

$$S = \frac{1}{|A|\,|B|}\sum_{i\in A}\sum_{j\in B} w_{ij},$$

where w_{ij} represents the weight of a functional connection (level of signal synchronization) between electrodes i and j. The group of electrodes A belongs to the frontal part of the hemisphere and group B to the temporal part of the hemisphere.

Functional connectivity was calculated in alpha, delta and theta frequency bands.

2.5.4. Analysis of functional brain networks

To calculate the functional connectomes, we used MNE-Connectivity package (Li et al., 2014). The connectomes were based on Vinck's debiased Weighted Phase Lag Index – dbWPLI (Vinck et al., 2011). This measure of connectivity was chosen because it is believed to have the highest stability and reliability when segmenting the EEG signal into 1-second epochs (Haartsen et al., 2020). Our connectomes are based on functional connections (coherence of EEG signals between individual electrodes), and the connectomes are undirected and weighted, meaning that the connections are bilateral and have a certain strength based on the signal coherence (from 0 to 1). To define the network characteristics, we calculated the clustering coefficient and global efficiency in both groups of subjects in the delta (0.5–4 Hz), theta (3–7 Hz), and alpha (8–13 Hz) frequency bands.

The **clustering coefficient** shows the number of connections between nodes that are neighbors of a specific node, as a proportion of all possible connections between all nodes in the network. It is a widely used measure that reflects the segmentation of the network into subunits (Bullmore and Sporns, 2009). It is calculated as:

$$C^w = \frac{1}{n}\sum_{i\in N} C_i^w = \frac{1}{n}\sum_{i\in N}\frac{2t_i^w}{k_i(k_i-1)},$$

where n represents the number of nodes (electrodes) in a connectome, k_i number of edges to the node i, t_i^w is the number of triplets around node i and C_i^w is the clustering coefficient of node i. The final metric value is the average value of all clustering coefficient values for all the nodes in the connectome.

The **global efficiency** of a network is the inverse of the average shortest path length in the network and is the most important measure estimating network integration (Latora and Marchiori, 2001). It is calculated as:

$$GE = \frac{1}{N(N-1)}\sum_{i}\ \sum_{\neq j}\frac{1}{w_{ij}},$$

where N represents the number of all electrodes (64) in w_{ij} the weight of connection between electrodes i in j.

2.6. Statistical analysis

For the analysis of the results, we used Bayesian statistics. All analyses were performed using the R programming language and the Stan tool – a state-of-the-art platform for conducting modern Bayesian statistical analyses (Stan Development Team, n.d.).

To analyze the differences between the test and control groups, we used a robust Bayesian t-test:

$$y|\mu,\ \sigma \sim Cauchy(\mu,\ \sigma).$$

All variables used Stan's default uninformative priors. We opted for a robust test to minimize the influence of outliers.

Since the sleep stages are correlated, we used the Bayesian Dirichlet model for this segment of the analysis:

$$\alpha \sim exponential(1),$$

$$y|\alpha \sim Dirichlet(\alpha),$$

where α represents the probability vector for a sleep stage for an individual participant.

To distinguish the reported Bayesian probabilities from frequentist p-values, we denote them with a capital letter P. Unlike p-values, our reported probabilities (P) directly describe the percentage with which we can claim that our hypotheses are true or not. Since we report probabilities as percentages, the probability that the opposite of our claim is true can be calculated as 100% - P.

We provide continuous probability measures for quantifying confidence in our results, which allows us to facilitate a more nuanced interpretation of the data. Following modern recommendations and statistical practices for reproducible research, we avoid the use of arbitrary significance thresholds (e.g. $p < 0.05$) as those can obscure marginal effects and are mapping a rich continuous specter into a simplified binary classifier. However, our reported values can be easily mapped to a binary 95% certainty framework ($P > 95\%$) if one desires to do so.

To quantify uncertainty in all our analyses, we used 95% confidence intervals.

All data, along with the source code for EEG data processing and statistical analyses are available in a public online repository: https://github.com/demsarjure/ped_smokers.

2.7. Ethical approval statement

This study was conducted in accordance with the Declaration of Helsinki and was approved by the Slovenian National Medical Ethics Committee, approval number 0120–376/2024–2711–3. Formal written informed consent was obtained from the parents or legal guardians of all neonatal participants prior to enrollment. The privacy and anonymity of the participants were strictly maintained throughout the data collection and analysis processes.

3. Results

3.1. Behavioral sleep assessment

Twenty-seven newborns were included in the analysis (19 female, 8 male), with 14 in the maternal smoking group (9 female, 5 male) and 13 in the maternal non-smoking group (10 female, 3 male).

When comparing the groups, we can state with a high probability that newborns of smoking mothers had a higher proportion of wakefulness compared to newborns of non-smoking mothers during the observation period – P = 96.83% [96.5%–97.48%].

Similarly, we can state with a moderate probability that newborns of smoking mothers had a higher proportion of drowsiness compared to newborns of non-smoking mothers – P = 94.35% [93.45%–94.85%].

When we compared REM duration between groups, newborns of smoking mothers seemed to have a lower proportion of REM sleep, but the probability was much lower – P = 74.93% [73.38%–75.93%]).

Comparing the duration of quiet sleep between groups, again it seemed that newborns of smoking mothers had a lower proportion of quiet sleep, but probability was only 84.5% [84.13%-86.25%]).

Fig. 6 illustrates the proportions of individual sleep stages during the observation period in newborns of smoking and non-smoking mothers.

3.2. EEG analysis

Twenty-four newborns were included in this analysis (9 female, 15

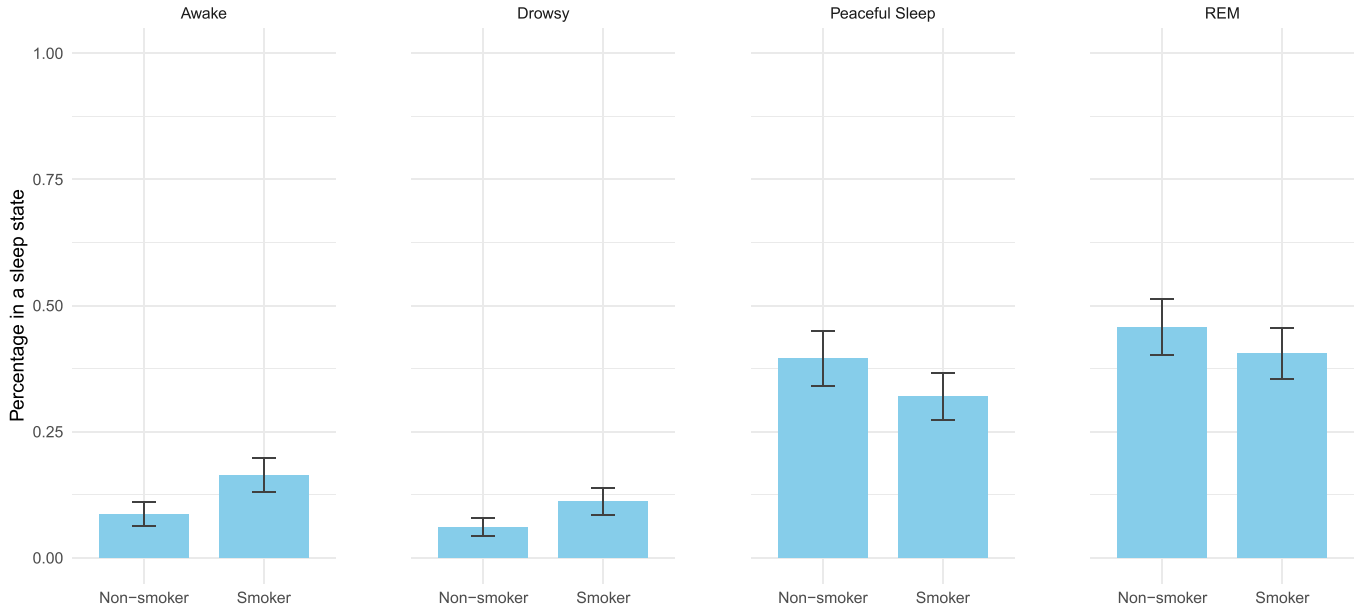

Fig. 6. Proportions of individual sleep stages during observation in newborns of smoking and non-smoking mothers. The columns show the average proportions and the error bars represent the 95% confidence interval.

male), with 12 in the maternal smoking group (4 female, 8 male) and 12 in the maternal non-smoking group (5 female, 7 male).

3.2.1. *Macrostructural sleep analysis*

The model used for automatic recognition of sleep stages from the EEG recording showed that newborns of non-smoking mothers seem to have a higher proportion of quiet sleep (a greater proportion of the *trace alternant* pattern) than newborns of smoking mothers – P = 87.58% [86.48%–88.4%]); see Fig. 7.

3.2.2. *Microstructural sleep analysis*

3.2.2.1. Spectral analysis. When analyzing the power of individual frequency bands, we found that there is a moderate probability that newborns of non-smoking mothers have greater power in the delta frequency band (P = 93.92% [93.4%–94.85%]), while there is a high probability that newborns of smoking mothers have greater power in the theta frequency band (P = 97.38% [96.95%–97.97%]) and a moderate probability that newborns of smoking mothers have greater power in the alpha frequency band (P = 91.95% [91%–92.65%]). The probability that the power in the beta frequency band is greater in newborns of smoking mothers is lower (P = 85.35% [83.93%–86.08%]). These results are presented in Fig. 8.

3.2.2.2. SEF 90. Based on our results, the probability that newborns of smoking mothers have a higher SEF 90 value is 88.72% [88.17%–90.03%]; see Fig. 9. This means that the cutoff frequency, below which 90% of brain activity is located, is higher in this group, therefore higher frequencies seem to dominate in the EEG recordings of newborns of smoking mothers.

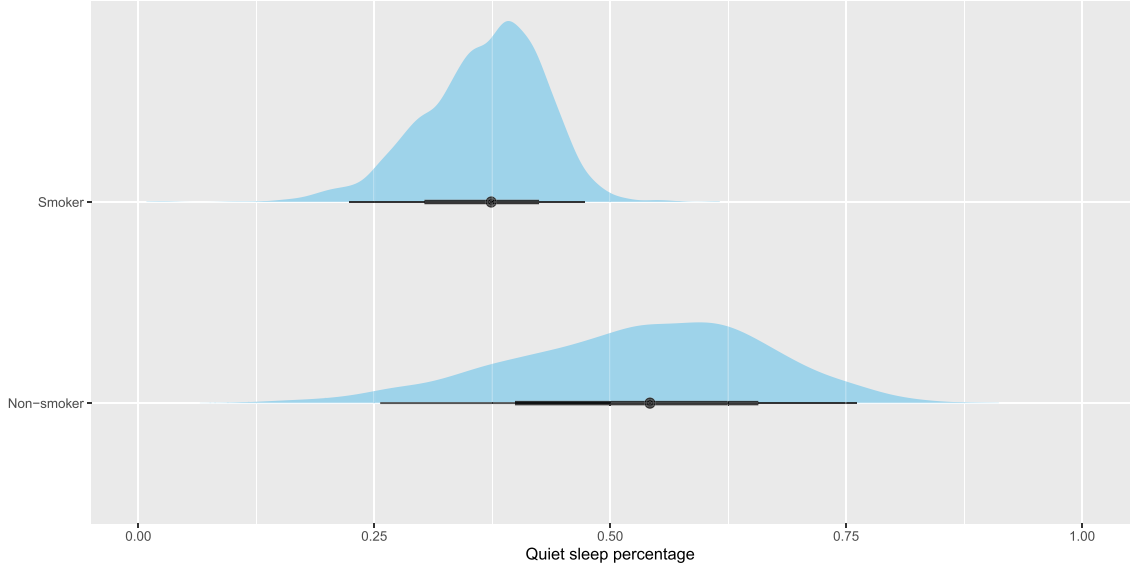

Fig. 7. The difference in the average proportion of quiet sleep (i.e., the *trace alternant* pattern) between newborns of smoking and non-smoking mothers. The dot represents the average value, the thick line represents the 66% confidence interval, the thin line represents the 95% confidence interval, and the blue area represents the distribution of values.

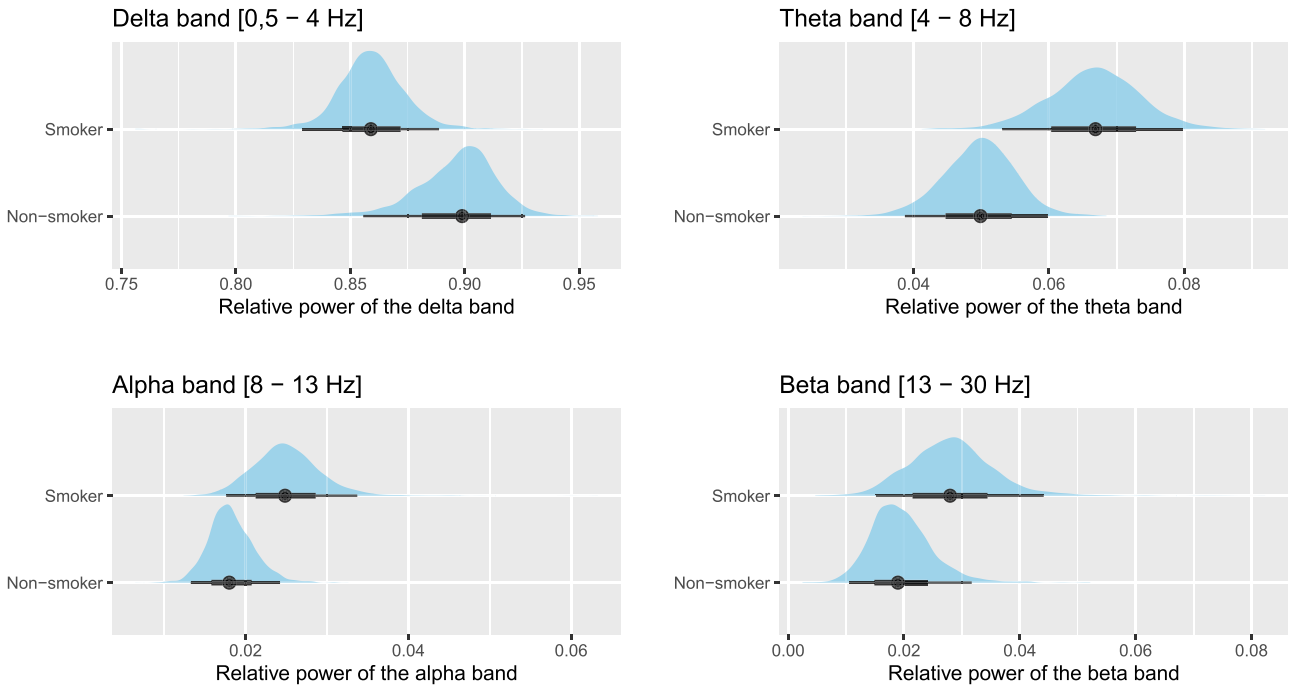

Fig. 8. The average power values for individual frequency bands for newborns of smoking and non-smoking mothers. The dot represents the average value, the thick line represents the 66% confidence interval, the thin line represents the 95% confidence interval, and the blue area represents the distribution of values.

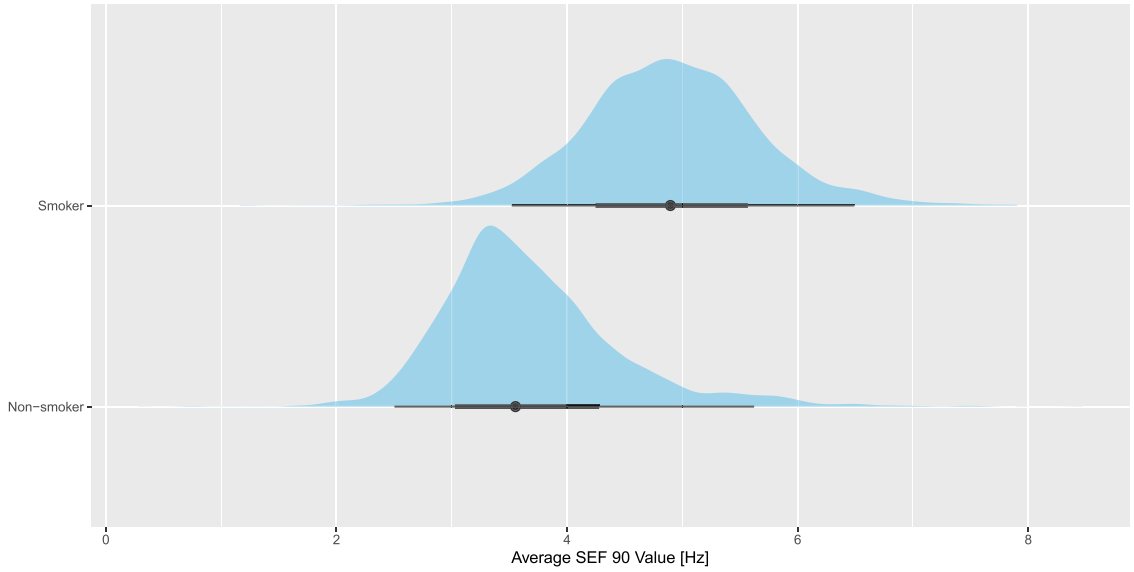

Fig. 9. The average SEF 90 value comparison between newborns of smoking and non-smoking mothers. The dot represents the average value, the bold line represents the 66% confidence interval, the thin line represents the 95% confidence interval, and the blue area represents the distribution of values.

Functional connectivity between temporal and frontal brain regions

Analysis of functional connectivity between fronto-temporal regions within individual hemispheres showed a moderate probability that newborns of non-smoking mothers have lower connectivity in the alpha frequency band (P = 90.08% [89.3%–91.13%]) and higher connectivity in the delta frequency band (P = 92.1% [91.2%–92.9%]); see Figs. 10 and 11. The changes in connectivity were present only in the right hemisphere.

3.2.2.3. Brain network analysis. Upon analyzing the network characteristics in the alpha, delta, and theta frequency bands, we discovered with high probability that newborns of non-smoking mothers have higher global efficiency of the brain network in the alpha frequency band (P = 97.7% [97.15%–98.12%]); see Fig. 12. In the other two frequency bands, the global efficiency did not differ between the groups. We also did not observe any difference in the average clustering coefficient between the groups in any frequency band.

4. Discussion

In this research article, we present evidence that maternal smoking influences newborn sleep architecture and brain activity, as reflected in both behavioral sleep observations and quantitative EEG measures. Newborns of smoking mothers exhibited a higher proportion of wakefulness and drowsiness, and a lower proportion of quiet sleep. Studies on the effects of indirect nicotine exposure on newborn sleep remain

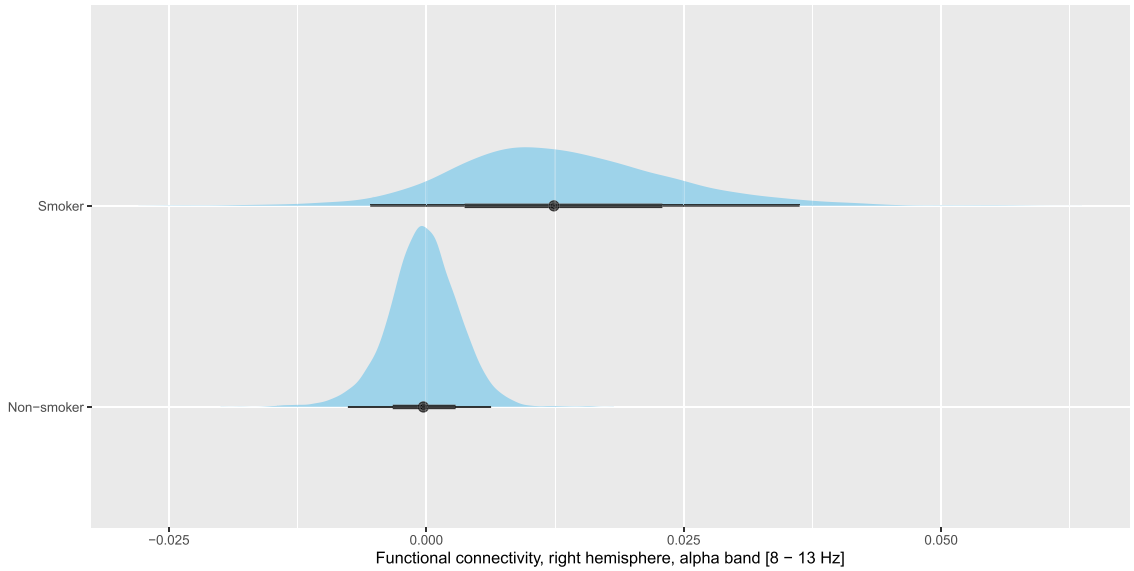

Fig. 10. The difference in the average value of fronto-temporal connectivity in the right hemisphere in the alpha frequency band between the groups of newborns of smoking and non-smoking mothers. The dot represents the average value, the thick line represents the 66% confidence interval, the thin line represents the 95% confidence interval, and the blue area represents the distribution of values.

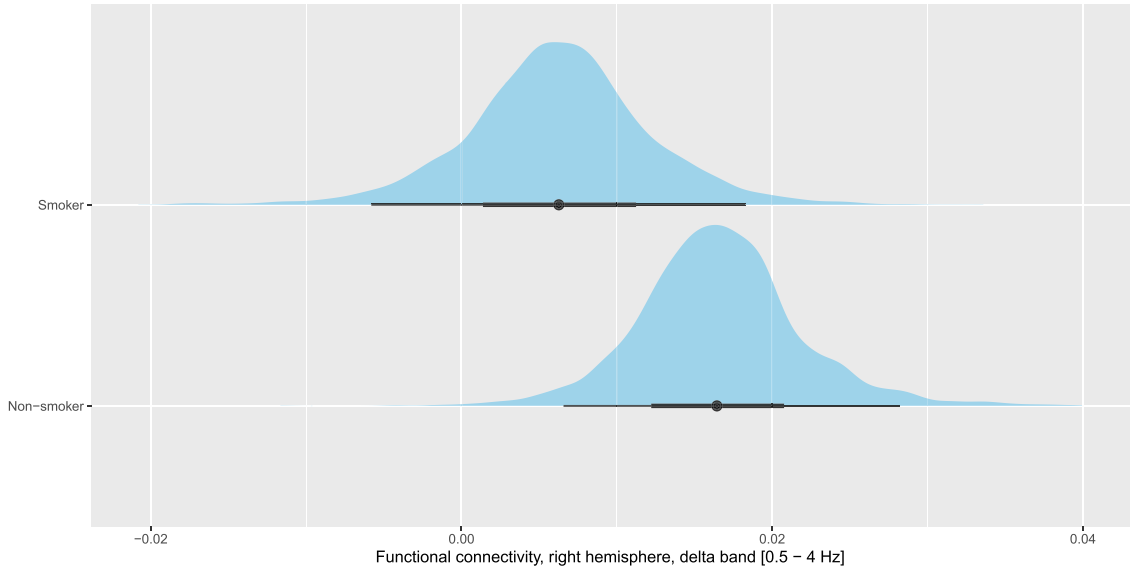

Fig. 11. The average value of fronto-temporal connectivity in the right hemisphere in the delta frequency band between the groups of newborns of smoking and non-smoking mothers. The dot represents the average value, the thick line represents the 66% confidence interval, the thin line represents the 95% confidence interval, and the blue area represents the distribution of values.

limited. We identified one relevant study that examined in utero nicotine exposure, showing that high levels of prenatal smoking were associated with decreased total sleep time, reduced quiet sleep, increased active sleep, and greater sleep fragmentation (Stephan-Blanchard et al., 2008). These findings are consistent with our results obtained through behavioral sleep assessment. Furthermore, we observed a trend suggesting that newborns of smoking mothers may have a lower proportion of REM sleep compared to those of non-smoking mothers; however, this result lacked statistical power and would require a larger sample size to make firmer conclusions.

When using an automated sleep stage detection model based on macrostructural EEG features (e.g., the presence of the *trace alternant* pattern), our analysis again demonstrated a lower percentage of quiet sleep in newborns of smoking mothers. The consistency of results between observational sleep assessment and automated EEG analysis strengthens the validity of our findings, as two distinct methodologies produced similar conclusions. A review by Abbasi et al. (2023) on automated neonatal sleep stage classification confirmed EEG as the most accurate method for sleep staging. However, some stages produce indistinguishable EEG signals, requiring integration of additional physiological signals to improve classification accuracy. While numerous studies have attempted to develop automated models for neonatal sleep staging, none have yet achieved high accuracy across all sleep stages. Existing models perform best at detecting quiet sleep, with reduced reliability for identifying REM sleep and drowsiness (Abbasi et al., 2023; Ansari et al., 2020; Ansari et al., 2018; Abbasi et al., 2020; Siddiqa et al., 2025).

The next focus of our study was the analysis of quantitative EEG characteristics. We found that newborns of smoking mothers had higher SEF 90 values, increased power in the theta and alpha frequency bands,

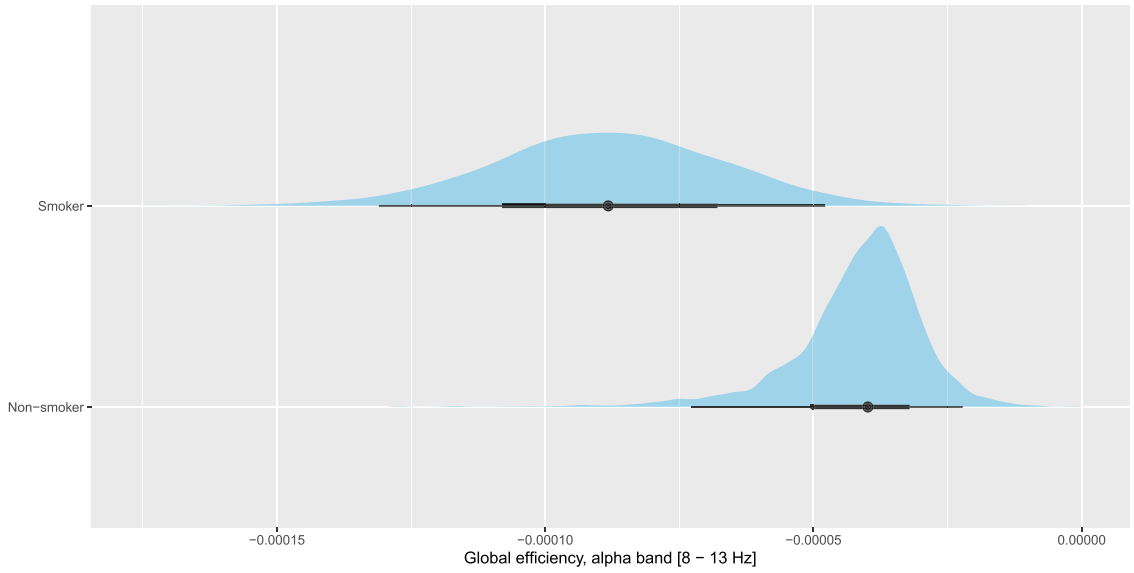

Fig. 12. The difference in the average value of global efficiency between the newborns of smoking and non-smoking mothers. The dot represents the average value, the bold line represents the 66% confidence interval, the thin line represents the 95% confidence interval, and the blue area represents the distribution of values.

and reduced power in the delta frequency band. These findings are in line with research on adults. For example, a resting-state EEG study by Lee et al. (2023) reported that chronic smokers exhibited significantly higher alpha power and alpha coherence, especially between the occipital and left frontotemporal regions, correlating with daily cigarette consumption. Similarly, Zhang et al. (2008) found that adult smokers had reduced delta power and increased alpha power during the early sleep period – patterns that were associated with complaints of restless sleep. Truong et al. (2021) reported delta power reduction to be linked to reduced sleep depth, and a dose-dependent relationship between smoking intensity and decreased delta power during non-REM sleep, along with increased alpha power. Although no prior studies have investigated the impact of indirect nicotine exposure on EEG features in newborns, emerging research suggests a link between EEG spectral characteristics and neurodevelopment. For instance, Castro Conde et al. (2020) found that newborns small for gestational age exhibited reduced delta power and increased alpha and beta power, which correlated with delayed brain maturation. Similarly, Shellhaas et al. (2014) reported that decreased delta power during quiet sleep was associated with abnormal neurological examination scores in critically ill neonates.

Additional quantitative EEG findings in our study revealed reduced global efficiency of the functional brain network in the alpha band and decreased frontotemporal connectivity in the right hemisphere within the delta band in newborns of smoking mothers. These results are supported by a systematic review by van 't Westende et al. (2022), which found that decreased sleep-induced connectivity and reduced coherence in the alpha and theta frequency bands were associated with poorer neurodevelopmental outcomes.

5. Limitations

Our study has some limitations. The most significant is the relatively small sample size, primarily due to difficulties in recruiting eligible participants, particularly given the low participation rate among smoking mothers. Despite this, the high probability values in our statistical analyses allowed us to draw meaningful conclusions. Another limitation lies in the use of observational sleep assessments. This challenge is not unique to our study, as no universally accepted method currently exists for reliably determining sleep stages in newborns through observation. A major concern is observer subjectivity, which can lead to inconsistencies. To minimize this, we implemented training sessions in which two researchers assessed the same subject simultaneously and discussed their findings. We also developed a standardized protocol for sleep stage classification based on previously published methodologies (de Groot et al., 2022) to further reduce variability. Conducting research with neonates in a clinical setting presents significant logistical challenges; however, we implemented several measures to minimize confounding variables. To reduce distress and artifact interference, the EEG cap was applied only once the infant reached a state of natural sleep and recording completed only if we observed no instances of arousal or irritability following placement. We must note that neonates prenatally exposed to tobacco often exhibit higher baseline irritability than the control group. To account for this, sessions were repeated when necessary to ensure a consistent, artifact-free recording of at least 30 min for every participant. Furthermore, because the observational and EEG assessments were conducted in separate sessions—and because the observational protocol remained identical for both groups (conducted over a three-hour inter-feeding period)—the risk of systemic bias is reduced. The fact that stage durations remained comparable across these distinct sessions further validates the stability of our findings.

6. Conclusions

Our study contributes novel insights into the indirect impact of maternal smoking during pregnancy and breastfeeding on newborn sleep architecture and brain function. Observational sleep assessment revealed that newborns of smoking mothers spent a greater proportion of time in wakefulness and drowsiness, and a smaller proportion in quiet sleep. A reduced percentage of quiet sleep was also confirmed using automated sleep stage detection based on EEG macrostructural features. Quantitative EEG analysis during sleep further demonstrated that newborns of smoking mothers exhibited increased power in the theta and alpha frequency bands, decreased power in the delta band, elevated spectral edge frequency (SEF 90), reduced global efficiency of the functional brain network in the alpha band, and diminished frontotemporal connectivity in the right hemisphere within the delta frequency band. By demonstrating both behavioral and neurophysiological alterations, this research provides a foundation for future studies and highlights the importance of early interventions targeting maternal health and smoking cessation.

CRediT authorship contribution statement

Jure Demšar: Software, Methodology, Formal analysis. **Alja Kavčič:** Writing – original draft, Validation, Supervision, Methodology, Conceptualization. **Žana Mlakar:** Writing – original draft, Data curation. **Maša Štihec:** Writing – original draft, Investigation, Data curation. **Soltirovska-Salamon Aneta:** Writing – review & editing, Methodology, Conceptualization.

Funding

The study was conducted within the national research program P3-0343 (Etiology, early detection and treatment of diseases in childhood and adolescence) and supported by the by the Slovenian Research and Innovation agency.

Declaration of Competing Interest

The authors declare that they have no known competing financial interests or personal relationships that could have appeared to influence the work reported in this paper.

Data availability

All data, along with the source code for EEG data processing and statistical analyses are available in a public online repository: https://github.com/demsarjure/ped_smokers.

References

van 't Westende, Geraedts, C., van Ramesdonk T, V.J., Dudink, J., Schoonmade, L.J., van der Knaap, M.S., et al., 2022. Neonatal quantitative electroencephalography and long-term outcomes: a systematic review. Dev. Med. Child Neurol. 64, 413–420. https://doi.org/10.1111/dmcn.15133.

Abbasi, S.F., Ahmad, J., Tahir, A., Awais, M., Chen, C., Irfan, M., et al., 2020. EEG-based neonatal sleep-wake classification using multilayer perceptron neural network. IEEE Access 8, 183025–183034. https://doi.org/10.1109/ACCESS.2020.3028182.

Abbasi, S.F., Abbas, A., Ahmad, I., Alshehri, M.S., Almakdi, S., Ghadi, Y.Y., et al., 2023. Automatic neonatal sleep stage classification: a comparative study. Heliyon 9. https://doi.org/10.1016/j.heliyon.2023.e22195.

Ansari, A.H., De Wel, O., Lavanga, M., Caicedo, A., Dereymaeker, A., Jansen, K., et al., 2018. Quiet sleep detection in preterm infants using deep convolutional neural networks. J. Neural Eng. 15, 066006. https://doi.org/10.1088/1741-2552/aadc1f.

Ansari, A.H., De Wel, O., Pillay, K., Dereymaeker, A., Jansen, K., Van Huffel, S., et al., 2020. A convolutional neural network outperforming state-of-the-art sleep staging algorithms for both preterm and term infants. J. Neural Eng. 17, 016028. https://doi.org/10.1088/1741-2552/ab5469.

Bullmore, E., Sporns, O., 2009. Complex brain networks: Graph theoretical analysis of structural and functional systems. Nat. Rev. Neurosci. 10, 186. https://doi.org/10.1038/nrn2575.

Castro Conde, J.R., González Campo, C., González González, N.L., Reyes Millán, B., González Barrios, D., Jiménez Sosa, A., et al., 2020. Assessment of neonatal EEG background and neurodevelopment in full-term small for their gestational age infants. Pedia Res. 88, 91–99. https://doi.org/10.1038/s41390-019-0693-0.

Davila, D.G., Hurt, R.D., Offord, K.P., Harris, C.D., Shepard, J.W., 1994. Acute effects of transdermal nicotine on sleep architedure, snoring, and sleep-disordered breathing in nonsmokers. Am. J. Respir. Crit. Care Med 150, 469–474.

De Beritto, T.V., 2020. Newborn sleep: patterns, interventions, and outcomes. Pedia Ann. 49, e82–e87. https://doi.org/10.3928/19382359-20200122-01.

Dereymaeker, A., Pillay, K., Vervisch, J., De Vos, M., Van Huffel, S., Jansen, K., et al., 2017. Review of sleep-EEG in preterm and term neonates. Early Hum. Dev. 113, 87–103. https://doi.org/10.1016/j.earlhumdev.2017.07.003.

Gramfort, A., Luessi, M., Larson, E., Engemann, D.A., Strohmeier, D., Brodbeck, C., et al., 2013. MEG and EEG data analysis with MNE-Python. Front Neurosci. 7, 267. https://doi.org/10.3389/fnins.2013.00267.

Grigg-Damberger, M.M., 2016. The visual scoring of sleep in infants 0–2 months of age. J. Clin. Sleep. Med. 12, 429–445. https://doi.org/10.5664/jcsm.5600.

de Groot, E.R., Bik, A., Sam, C., Wang, X., Shellhaas, R.A., Austin, T., et al., 2022. Creating an optimal observational sleep stage classification system for very and extremely preterm infants. Sleep. Med. 90, 167–175. https://doi.org/10.1016/j.sleep.2022.01.020.

Haartsen, R., van der Velde, B., Jones, E.J.H., Johnson, M.H., Kemner, C., 2020. Using multiple short epochs optimises the stability of infant EEG connectivity parameters. Sci. Rep. 10, 1–13. https://doi.org/10.1038/s41598-020-68981-5.

Htoo, A., Talwar, A., Feinsilver, S.H., Greenberg, H., 2004. Smoking and sleep disorders. Med. Clin. North Am. 88, 1575–1591. https://doi.org/10.1016/j.mcna.2004.07.003.

Jaehne, A., Unbehaun, T., Feige, B., Lutz, U.C., Batra, A., Riemann, D., 2012. How smoking affects sleep: a polysomnographical analysis. Sleep. Med. 13, 1286–1292. https://doi.org/10.1016/j.sleep.2012.06.026.

Jas, M., Engemann, D.A., Bekhti, Y., Raimondo, F., Gramfort, A., 2017. Autoreject: Automated artifact rejection for MEG and EEG data. Neuroimage 159, 417–429. https://doi.org/10.1016/j.neuroimage.2017.06.030.

Latora, V., Marchiori, M., 2001. Efficient behavior of small-world networks. Phys. Rev. Lett. 87, 198701. https://doi.org/10.1103/PhysRevLett.87.198701.

Lee, H., Jeon, Y., Yoo, C., Seon, H.Y., Park, J., Hwang, M., et al., 2023. Persistent impacts of smoking on resting-state EEG in male chronic smokers and past-smokers with 20 years of abstinence. Sci. Rep. 13. https://doi.org/10.1038/s41598-023-29547-3.

Li, A., Engemann, D.A., Jas, M., Brooks, T., Quentin, R., van Vliet, M., , 2014. MNE-Connectivity: A Python package for computing connectivity measures on MEG/EEG/iEEG data 2014:667–676.667676.

Rass, O., Ahn, W.Y., O'Donnell, B.F., 2016. Resting-state EEG, impulsiveness, and personality in daily and nondaily smokers. Clin. Neurophysiol. 127, 409–418. https://doi.org/10.1016/j.clinph.2015.05.007.

Raurale, S.A., Boylan, G.B., Lightbody, G., O'Toole, J.M., 2020. Identifying trace alternant activity in neonatal EEG using an inter-burst detection approach. 42nd Annual International Conference of the IEEE Engineering in Medicine & Biology Society, pp. 5984–5987.

Seth, P., Cheeta, S., Tucci, S., File, S.E., 2002. Nicotinic-serotonergic interactions in brain and behaviour, pp. 795–805.

Shellhaas, R., Burns, J., Barks, J., Chervin, R., 2014. Quantitative sleep stage analyses as a window to neonatal neurologic function. Neurology (5), 390–395.

Siddiqa, H.A., Qureshi, M.F., Khurshid, A., Xu, Y., Wang, L., Abbasi, S.F., et al., 2025. EEG electrode setup optimization using feature extraction techniques for neonatal sleep state classification. Front Comput. Neurosci. 19. https://doi.org/10.3389/fncom.2025.1506869.

Stan Development Team. Stan Modeling Language Users Guide and Reference Manual n. d. ⟨https://mc-stan.org⟩.

Stephan-Blanchard, E., Telliez, F., Leke, A., Djeddi, D., Bach, V., Libert, J., et al., 2008. The influence of in utero exposure to smoking on sleep patterns in preterm neonates. Sleep (12), 1683–1689.

Truong, M.K., Berger, M., Haba-Rubio, J., Siclari, F., Marques-Vidal, P., Heinzer, R., 2021. Impact of smoking on sleep macro– and microstructure. Sleep. Med 84, 86–92. https://doi.org/10.1016/j.sleep.2021.05.024.

Vinck, M., Oostenveld, R., Van Wingerden, M., Battaglia, F., Pennartz, C.M.A., 2011. An improved index of phase-synchronization for electrophysiological data in the presence of volume-conduction, noise and sample-size bias. Neuroimage 55, 1548–1565. https://doi.org/10.1016/j.neuroimage.2011.01.055.

Yolton, K., Xu, Y., Khoury, J., Succop, P., Lanphear, B., Beebe, D.W., et al., 2010. Associations between secondhand smoke exposure and sleep patterns in children. Pediatrics 125. https://doi.org/10.1542/peds.2009-0690.

Zhang, L., Samet, J., Caffo, B., Punjabi, N.M., 2006. Cigarette smoking and nocturnal sleep architecture. Am. J. Epidemiol. 164, 529–537. https://doi.org/10.1093/aje/kwj231.

Zhang, L., Samet, J., Caffo, B., Bankman, I., Punjabi, N.M., 2008. Power spectral analysis of EEG activity during sleep in cigarette smokers. Chest 133, 427–432. https://doi.org/10.1378/chest.07-1190.